Te-As-Se glass microstructured optical fiber for the middle infrared

Frédéric Désévédavy,[1,5] Gilles Renversez,[4] Johann Troles,[1,*] Laurent Brilland,[2] Patrick Houizot,[1] Quentin Coulombier,[1] Frédéric Smektala,[3] Nicholas Traynor,[2] and Jean-Luc Adam[1]

[1]Equipe Verres et Céramiques, UMR-CNRS 6226, Science Chimiques de Rennes, Université de Rennes I, 35042 Rennes Cedex, France,

[2]Plate-Forme d'Etude et de Recherches sur les Fibres Optiques Spéciales, 11, rue Louis de Broglie, 22300 Lannion, France

[3]Institut Carnot de Bourgogne, ICB UMR 5209 CNRS-Université de Bourgogne, 9 Avenue A. Savary, BP 47870, 21078 Dijon cedex, France

[4]Institut Fresnel, UMR CNRS 6133, Université d'Aix-Marseille, 13397 Marseille, France

[5]frederic.desevedavy@polymtl.ca

*Corresponding author: johann.troles@univ-rennes1.fr

Received 30 March 2009; accepted 26 May 2009;
posted 17 June 2009 (Doc. ID 109392); published 30 June 2009

We present the first fabrication, to the best of our knowledge, of chalcogenide microstructured optical fibers in Te-As-Se glass, their optical characterization, and numerical simulations in the middle infrared. In a first fiber, numerical simulations exhibit a single-mode behavior at 3.39 and 9.3 μm, in good agreement with experimental near-field captures at 9.3 μm. The second fiber is not monomode between 3.39 and 9.3 μm, but the fundamental losses are 9 dB/m at 3.39 μm and 6 dB/m at 9.3 μm. The experimental mode field diameters are compared to the theoretical ones with a good accordance.

OCIS codes: 160.2750, 060.2390, 060.2270, 060.2280.

1. Introduction

Since the pioneering work of Russell [1] and Birks [2], microstructured optical fibers (MOFs) have formed a new class of optical fibers. The arrangement of the airholes along the transverse section of the fiber leads to unique optical properties such as broadband single-mode guidance [3], adjustable dispersion [4], large or small area, and nonlinear properties [5,6]. Up to now, the majority of the MOFs developed are made from silica glass and studied in the visible and the near-infrared wavelengths. For longer wavelengths, infrared materials are required. For example, the chalcogenide glass fibers based on selenium, tellurium, and arsenic present a broadband window in the middle infrared from 2 to 11 μm. The achievement of single-mode guiding in the mid-infrared is complex. Only a few studies are available: some of them concern step index and microstructured chalcogenide fibers [7–11], and others are about integrated waveguides, also in chalcogenide glass [12]. Step index single-mode fibers and microstructured fibers made of silver halide polycrystals based in Ag-Cl-Br have also been obtained [13,14]. In the present study, we focus on chalcogenide MOFs. Our work is motivated by the wide field of applications such as propagation of high intensity laser beams (i.e., CO_2) [15], broadband sources, sensors, and spatial filtering for realization

0003-6935/09/193860-06$15.00/0

of a nulling interferometer for exoplanet detection (DARWIN project) [7,16].

In Section 2 the fabrication and characterization are described. Two TAS (tellurium, arsenic, and selenium) MOFs with different designs have been elaborated by the "stack and draw" procedure. In Section 3, the optical characterization of the two TAS MOFs with optical losses and mode field diameter of the fundamental mode are compared to numerical simulations. The single-mode behavior of the two fibers is also investigated by near-field capture at 3.39 and 9.3 μm. Our results, including the single-mode behavior and the overall losses of the studied TAS MOFs, are discussed in Section 4.

2. MOF Fabrication and Characterization Procedures

The nominal composition of the chalcogenide glass we studied is $Te_{20}As_{30}Se_{50}$ (TAS). It is transparent between 2 and 18 μm on a bulk piece, and its refractive index varies from 2.96 at 2 μm to 2.90 at 12 μm [7,17].

The material losses of the MOFs presented in this study are measured on a single index fiber of the same glass by the cutback method; they are equal to 1.5 dB/m at 9.3 μm and 2.5 dB/m at 3.39 μm. The MOFs in TAS glass presented here are made of three rings and fabricated by the "stack and draw" technique which is compatible with chalcogenide glasses; the technical realization is described in [8,11]. With these glasses, three rings are sufficient to guarantee theoretical guiding losses below material ones [8]. We fabricated two different TAS MOFs, and we differentiate them by the following labels: TAS MOF #1 and TAS MOF #2.

Optical measurements are made on TAS microstructured fibers using near-field microscopy. A gallium metal coating is applied to inhibit cladding mode guidance. A monochromatic light ($\lambda = 9.3\,\mu$m or $\lambda = 3.39\,\mu$m) going through a Zn–Se lens is launched in a TAS MOF micropositioned in the three directions of space. The sources we used are, respectively, a CW CO_2 laser and a CW He–Ne laser, both TEM_{00}. The image of the fiber output is visualized on a 3–5 μm or an 8–12 μm forward looking infrared (FLIR) camera, depending on the laser, as shown later in Figs. 3–6.

The optical losses in the TAS MOF are measured by the cutback method. The typical length of fibers used is a couple of meters at 9.3 μm and 1 m at 3.39 μm. For the measure at 9.3 μm the detector used is a nitrogen-cooled mercury cadmium telluride (MCT) detector that has detectivity in the spectral range from 1 to 20 μm. At 3.39 μm the output intensity is measured by a noncooled preamplified InSb detector that has detectivity in the spectral range from 1 to 5 μm.

3. Experimental and Modeling Results

Figure 1 shows the transverse section of the TASMOF#1. The hole diameter d is equal to 6 μm and the pitch Λ is 17 μm (distance between two adjacent hole centers), the outer diameter being 350 μm. One hole is missing in the third ring of holes because of a capillary collapse during the drawing process. It has been shown that a MOF is endlessly single mode when the ratio d/Λ is under 0.42; this has been demonstrated theoretically and experimentally for silicalike glasses [3,18,19]. Furthermore, this limit is conserved for a large structure, whatever the index of refraction, including chalcogenide glass [20].

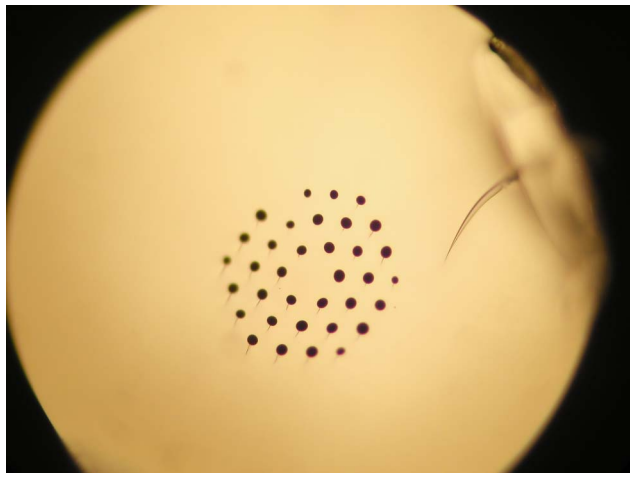

Fig. 1. (Color online) Microscope photo of TAS MOF # 1 ($\Phi_{\text{fiber}} = 350\,\mu$m, $d = 6\,\mu$m, $\Lambda = 17\,\mu$m, and $d/\Lambda = 0.35$).

As the ratio d/Λ is under 0.42, theoretically this MOF is endlessly single mode. However, as there are only three rings of holes, one has to take into account the finite size effects [20].

In order to study the single-mode guidance of this fiber at 9.3 μm, numerical simulation has been performed by use of the multipole method [19]. A MOF with the same geometry (number of rings, d, pitch, and the interstitial holes) has been modeled. The refractive index for a large range of wavelengths is given by [7,17], $n = 2.9294 \pm 2 \times 10^{-4}$ at 3.39 μm and $n = 2.9094 \pm 2 \times 10^{-4}$ at 9.3 μm. Table 1 reports the experimental losses, the calculated losses of the fundamental mode, and only the calculated ones of the second mode for the TAS MOF#1. The simulations take into account the measured materials losses (1.5 dB/m at 9.3 μm and 2.5 dB/m at 3.39 μm).

With the goal of reducing optical losses, we fabricated another TAS MOF with opened interstices in order to decrease the capillary interfaces that are scattering defect sources responsible for losses [21].

Table 1. Theoretical and Experimental Losses of the TAS MOF #1

	Theoretical		Experimental
Wavelength	Fundamental Mode Guiding losses (dB/m)	Second Mode Guiding Losses (dB/m)	Fundamental Mode Losses (dB/m)
3.39 μm	2.51	230	>20
9.3 μm	1.61	750	>20

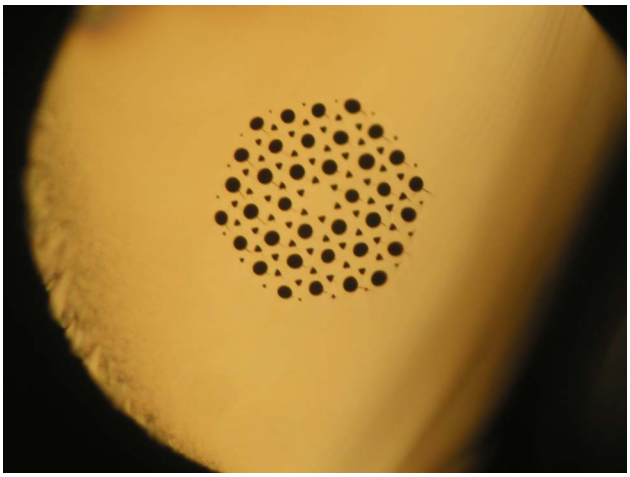

Fig. 2. (Color online) Microscope photo of TAS MOF # 2 ($\Phi_{\text{fiber}} = 255\,\mu\text{m}$, $d = 6.14\,\mu\text{m}$, and $\Lambda = 13.77\,\mu\text{m}$).

The cross section of this TAS MOF #2 is presented by Fig. 2. One can observe that the geometry is well controlled. The three rings and the interstitial holes are regulars. The average size of these interstitial holes is around $2.7\,\mu\text{m}$. Interstitial holes can be closed or opened depending of the pressure conditions during the drawing process. The TAS MOF #2 attenuation at $9.3\,\mu\text{m}$ is measured to be $6 \pm 1\,\text{dB/m}$; at $3.39\,\mu\text{m}$ it is worth $9 \pm 1\,\text{dB/m}$. If the interstitials holes are collapsed, the losses of the fibers reach 20–30 dB/m [21].

Optical experiments reported below are performed on the TAS MOF #2 (Fig. 2). The outer diameter is $255\,\mu\text{m}$, the diameter of the holes is $6.14\,\mu\text{m}$, the pitch or Λ is $13.77\,\mu\text{m}$, and the ratio d/Λ is around 0.44.

The near-field images of the fiber output are visualized at $9.3\,\mu\text{m}$ (Fig. 3) and at $3.39\,\mu\text{m}$ (Fig. 4). The output profiles can be accurately fitted with Gaussian functions, as illustrated in Figs. 3 and 4. These profiles show that the TAS MOF# 2 can present

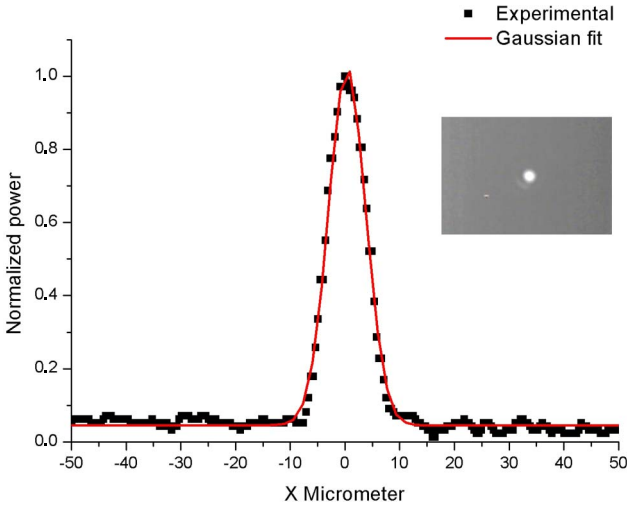

Fig. 3. (Color online) Experimental profile of the output beam at $9.3\,\mu\text{m}$ in TAS MOF #2 together with its Gaussian fit and in the inset a near-field observation of the guided mode at $9.3\,\mu\text{m}$.

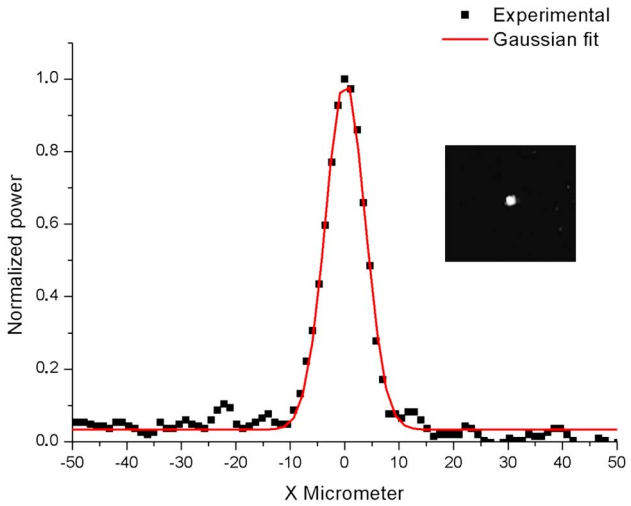

Fig. 4. (Color online) Experimental profile of the output beam at $3.39\,\mu\text{m}$ in TAS MOF#2 together with its Gaussian fit and in the inset a near-field observation of the guided mode at $3.39\,\mu\text{m}$.

single-mode behavior at $3.39\,\mu\text{m}$ and $9.3\,\mu\text{m}$. The mode field distributions, although slightly distorted, show no evidence of the structure associated with higher-order modes.

This fiber has been modeled, taking into account the materials losses, using a method other than the one used for the TAS MOF #1, i.e., the finite element method in order to deal with the interstitial holes. The results are summarized in Table 2.

4. Discussion

Theoretical calculations show that TAS MOF #1 is not rigorously single mode (see Table 1). However, guiding losses of the core guided second mode at $9.3\,\mu\text{m}$ are calculated to be greater than 750 dB/m, whereas the fundamental ones are found to be 1.61 dB/m. This means that from a practical point of view this fiber is single mode because it is not possible to detect a second mode with such high losses. One can note that this result is also true at a shorter wavelength, like $3.39\,\mu\text{m}$ (Table 2).

The theoretical results are confirmed by the experience at $9.3\,\mu\text{m}$, as shown by Fig. 5 representing the output profile of $9.3\,\mu\text{m}$ waveguiding. The output profile is accurately fitted with a Gaussian function, whatever the chosen injection condition, meaning single-mode behavior.

The attenuation at $9.3\,\mu\text{m}$ of TAS MOF #1 is estimated to be higher than 20 dB/m; as one can see in Table 1, there is an excess of losses between theoretical guiding losses and experimental ones. Keeping in mind the material losses are measured to be 1.5 dB/m at $9.3\,\mu\text{m}$ and 2.5 dB/m at $3.39\,\mu\text{m}$, the excess of loss cannot be quietly attributed to the material. Hence we believe the drawing process is responsible for it [22].

Concerning the single-mode TAS MOF #2, the simulations taking into account the material losses show that several modes are confined in the core

Table 2. Theoretical and Experimental Optical Properties of the TAS MOF #2

	Theoretical					Experimental	
	Fundamental Mode			Second Mode		Fundamental Mode	
Wavelength	Losses (dB/m)	MFD (μm)	External angle (°)	Losses (dB/m)	External angle[a] (°)	Losses (dB/m)	MFD[b] (μm)
3.39 μm	4.64	12.3 ± 0.3	9.31	4.65	14.24	9 ± 1	13.5 ± 2
9.3 μm	1.51	12.9 ± 0.3	24.98	1.62	38.98	6 ± 1	13.6 ± 2

[a]The external angle is obtained from the computed propagation constant of the studied mode for an external medium with a refractive index equal to one.

[b]The experimental measurement of the MFD is not accurate enough to make any difference between a diameter going through opposite summits of the hexagon and another one going through the middle of opposite faces.

structure. In our case the simulations show that the losses of the fundamental and the second modes present nearly the same losses (see Table 2). So theoretically the fiber is not single mode. For the shorter wavelength at 3.39 μm, a single-mode (Fig. 4) and a multimode behavior (Fig. 6) have been observed depending on the condition of the injection. Indeed, in Fig. 6, we can observe in the near-field capture that the profile is far from Gaussian. But, experimentally at 9.3 μm, even by changing the conditions of the injection, only the fundamental mode can be observed.

This disagreement between the experimental results and the theoretical ones can probably be explained by the high numerical aperture of the second mode, near 39° of divergence (Table 2). Indeed, if we consider this large angle, the experimental near-field setup cannot well observe the contribution of this mode. At 3.39 μm the divergence of the second mode is smaller and permits us to observe the fundamental and the second modes together (Fig. 6).

The calculations also give the theoretical mode-field diameter (MFD) of the fundamental mode for the two considered wavelengths of 3.39 and 9.3 μm (Table 1). The MFD has been calculated around 12.3 μm ($\pm 0.3\,\mu$m) at 3.39 μm and around 12.9 μm ($\pm 0.3\,\mu$m) at 9.3 μm (depending on the cutting axis). The MFD of TAS MOF #2 at $1/e^2$ of maximum intensity of the fundamental mode is measured using a Gaussian curve fitted to the mode profile (see Figs. 3 and 4). Experimentally, the MFDs at 3.39 and 9.3 μm, measured by near-field measurements, are 13.5 μm ($\pm 2\,\mu$m) and 13.6 μm ($\pm 2\,\mu$m), respectively. With regard to the experimental errors, the experimental values are in agreement with the theoretical ones.

Simulation results also demonstrate that the limiting factor for the overall fundamental mode losses is the material one. According to the intrinsic material losses, the transmission can be improved by using TAS glass with lower losses. It is worthwhile to mention that with further purifications we obtained a single index TAS fiber with overall loss values equal to 0.4 dB/m at 9.3 μm and 0.7 dB/m at 3.39 μm [23] compared to 1.5 dB/m and 2.5 dB/m, respectively, of the glass used for the realization of the TAS MOF #2. Nevertheless, we believe that a part of the loss is due to shaping the glass during fabrication of the MOFs [21]. More precisely, temperature and gas pressure parameters during the jacketing and the drawing are of great importance. Indeed during these steps such defects as bubbles or crystals are likely created, and control of the temperature and gas pressure allow us to decrease

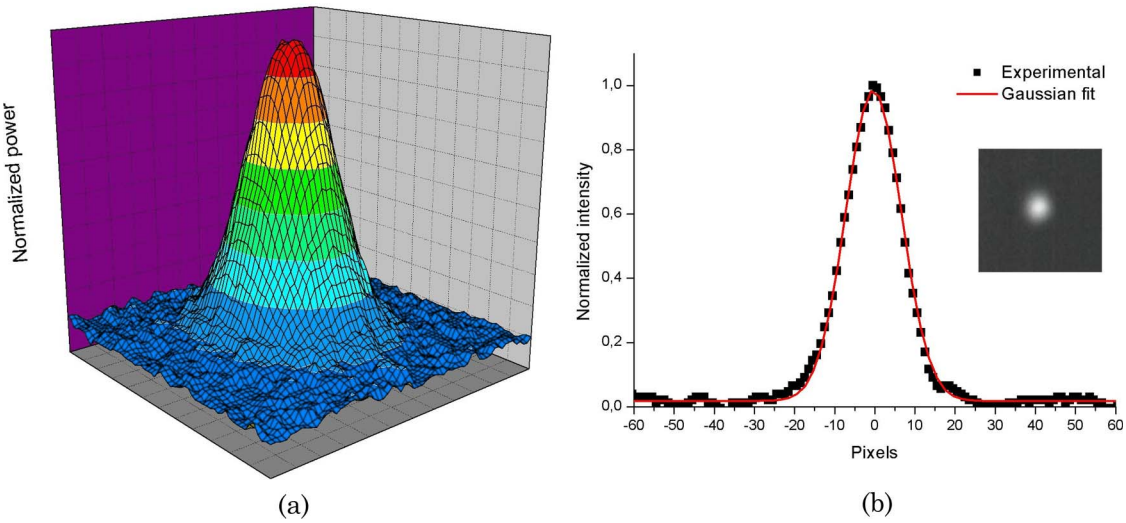

Fig. 5. (Color online) Experimental profile of the output beam at 9.3 μm in TAS MOF #1: (a) 3D view and (b) cut of the 3D profile together with its Gaussian fit, and in the inset a near-field observation of the guided mode.

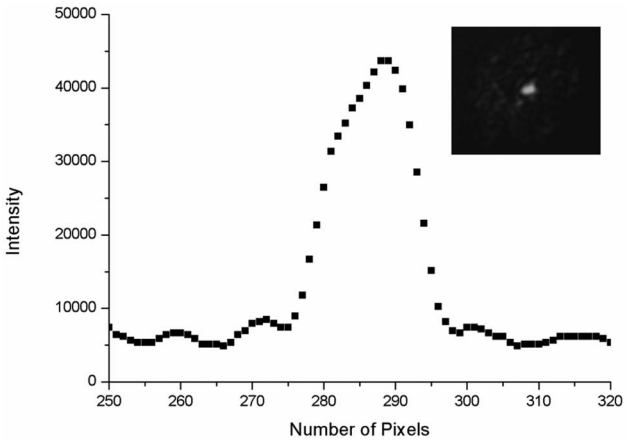

Fig. 6. Observation of multimode behavior in TAS MOF#2 at 3.39 μm.

or avoid their formation. Such improvements are currently under investigation to avoid such faults.

5. Conclusion

Two chalcogenide MOFs composed of Te, Se, and As have been realized by the stack and draw technique.

The simulations have shown that more than one mode can be confined in the core of the two fibers at 3.39 and 9.3 μm. In the first case, TAS MOF #1, the computed guiding losses of the second mode in the mid-infrared are higher than 750 dB/m, meaning that in practice TAS MOF #1 is single mode in this wavelength range. Concerning the second fiber, TAS MOF #2, for the first time to our knowledge, a regular fundamental mode profile has been observed in a chalcogenide MOF in the middle infrared both at 3.39 and 9.3 μm. The comparisons of the calculated and experimental fundamental mode diameters are in good agreement. The transmission losses of the TAS MOF #2 have been measured around 6 and 9 dB/m at 9.3 and 3.39 μm, respectively. Improvement in the glass purification and in the drawing processes are in progress to reduce overall losses under 1 dB/m and to get endlessly single-mode behavior. Sensors, spatial filters, and power delivery are potential applications of those types of fibers.

We acknowledge the French Délégation Générale pour l'Armenent (contracts 05.43.053 and 07.34.031) for its financial support.

References

1. P. St. J. Russell, "Photonic crystal fibers," Science **299**, 358–362 (2003).
2. T. A. Birks, P. J. Roberts, P. St. J. Russell, D. M. Atkin, and T. J. Shepherd, "Full 2-D photonic bandgaps in silica/air structures," Electron. Lett. **31**, 1941–1943 (1995).
3. T. A. Birks, J. C. Knight, and P. St. J. Russell, "Endlessly single-mode photonic crystal fiber," Opt. Lett. **22**, 961–963 (1997).
4. G. Renversez, B. Kuhlmey, and R. McPhedran, "Dispersion management with microstructured optical fibers: ultraflattened chromatic dispersion with low losses," Opt. Lett. **28**, 989–991 (2003).
5. T. M. Monro and D. J. Richardson, "Holey optical fibres: fundamental properties and device applications," C. R. Physique **4**, 175–186 (2003).
6. K. Schuster, J. Kobelke, S. Grimm, A. Schwuchow, J. Kirchhof, H. Bartelt, A. Gebhardt, P. Leproux, V. Couderc, and W. Urbanczyk, "Microstructured fibers with highly nonlinear materials," Opt. Quantum Electron. **39**, 1057–1069 (2007).
7. P. Houizot, C. Boussard-Pledel, A. J. Faber, L. K. Cheng, B. Bureau, P. A. Van Nijnatten, W. L. M. Gielesen, J. P. do Carmo, and J. Lucas, "Infrared single mode chalcogenide glass fiber for space," Opt. Express **15**, 12529–12538 (2007).
8. L. Brilland, F. Smektala, G. Renversez, T. Chartier, J. Troles, T. N. Nguyen, N. Traynor, and A. Monteville, "Fabrication of complex structures of holey fibers in chalcogenide glass," Opt. Express **14**, 1280–1285 (2006).
9. E. M. Dianov, V. G. Plotnichenko, Y. N. Pyrkov, I. V. Smol'nikov, S. A. Koleskin, G. G. Devyatykh, M. F. Churbanov, G. E. Snopatin, I. V. Skripachev, and R. M. Shaposhnikov, "Single-mode As-S glass fibers," Inorg. Mater. **39**, 627–630 (2003).
10. R. Mossadegh, J. S. Sanghera, D. Schaafsma, B. J. Cole, V. Q. Nguyen, P. E. Miklos, and I. D. Aggarwal, "Fabrication of single-mode chalcogenide optical fiber," J. Lightwave Technol. **16**, 214–217 (1998).
11. F. Désévédavy, G. Renversez, L. Brilland, P. Houizot, J. Troles, Q. Coulombier, F. Smektala, N. Traynor, and J.-L. Adam, "Small-core chalcogenide microstructured fibers for the infrared," Appl. Opt. **47**, 6014–6021 (2008).
12. N. Ho, M. C. Phillips, H. Qiao, P. J. Allen, K. Krishnaswami, B. J. Riley, T. L. Myers, and N. C. Anheier, "Single-mode low-loss chalcogenide glass waveguides for the mid-infrared," Opt. Lett. **31**, 1860–1862 (2006).
13. L. N. Butvina, O. V. Sereda, E. M. Dianov, N. V. Lichkova, and V. N. Zagorodnev, "Single-mode microstructured optical fiber for the middle infrared," Opt. Lett. **32**, 334–336 (2007).
14. E. Rave, P. Ephrat, M. Goldberg, E. Kedmi, and A. Katzir, "Silver halide photonic crystal fibers for the middle infrared," Appl. Opt. **43**, 2236–2241 (2004).
15. J. H. V. Price, T. M. Monro, H. Ebendorff-Heidepriem, F. Poletti, V. Finazzi, J. Y. Y. Leong, P. Petropoulos, J. C. Flanagan, G. Brambilla, X. Feng, and D. J. Richardson, "Non-silica microstructured optical fibers for mid-IR supercontinuum generation from 2 μm–5 μm," Proc. SPIE **6102**, 61020A (2006).
16. J. C. Flanagan, D. J. Richardson, M. J. Foster, and I. Bakalski, "Microstructured fibers for broadband wavefront filtering in the mid-IR," Opt. Express **14**, 11773–11786 (2006).
17. L. G. Aio, A. M. Efimov, and V. F. Kokorina, "Refractive-index of chalcogenide glasses over a wide range of compositions," J. Non-Cryst. Solids **27**, 299–307 (1978).
18. L. Labonte, D. Pagnoux, P. Roy, F. Bahloul, M. Zghal, G. Melin, E. Burov, and G. Renversez, "Accurate measurement of the cutoff wavelength in a microstructured optical fiber by means of an azimuthal filtering technique," Opt. Lett. **31**, 1779–1781 (2006).
19. F. Zolla, G. Renversez, A. Nicolet, B. Kuhlmey, S. Guenneau, and D. Felbacq, *Foundations of Photonic Crystal Fibres* (Imperial College Press, 2005), Section 7.2.
20. G. Renversez, F. Bordas, and B. T. Kuhlmey, "Second mode transition in microstructured optical fibers: determination of the critical geometrical parameter and study of the matrix refractive index and effects of cladding size," Opt. Lett. **30**, 1264–1266 (2005).
21. L. Brilland, J. Troles, P. Houizot, F. Desevedavy, Q. Coulombier, G. Renversez, T. Chartier, T. N. Nguyen,

J. L. Adam, and N. Traynor, "Interfaces impact on the transmission of chalcogenides photonic crystal fibres," J. Ceram. Soc. Jpn. **116**, 1024–1027 (2008).
22. L. Brilland, P. Houizot, J. Troles, F. Desevedavy, Q. Coulombier, T. N. Nguyen, and T. Chartier, "Improvement of the transmission of chalcogenide photonic crystal fibres: observation of self phase modulation spectral broadening," presented at the 34th European Conference and Exhibition on Optical Communication, Brussels, Belgium, 21–25 September 2008.
23. V. S. Shiryaev, J. L. Adam, X. H. Zhang, C. Boussard-Pledel, J. Lucas, and M. F. Churbanov, "Infrared fibers based on Te-As-Se glass system with low optical losses," J. Non-Cryst. Solids **336**, 113–119 (2004).